

Mutual interplay between IL-17-producing $\gamma\delta$ T cells and microbiota orchestrates oral mucosal homeostasis

Anneke Wilharm^{a,1}, Yaara Tabib^{b,1}, Maria Nassar^b, Annika Reinhardt^{a,2}, Gabriel Mizraji^c, Inga Sandrock^a, Oded Heyman^c, Joana Barros-Martins^a, Yuval Aizenbud^b, Abed Khalaileh^d, Luba Eli-Berchoer^b, Eran Elinav^e, Asaf Wilensky^c, Reinhold Förster^a, Herve Bercovier^f, Immo Prinz^{a,3,4}, and Avi-Hai Hovav^{b,3,4}

^aInstitute of Immunology, Hannover Medical School, 30625 Hannover, Germany; ^bInstitute of Dental Sciences, Faculty of Dental Medicine, Hebrew University, 9190501 Jerusalem, Israel; ^cDepartment of Periodontology, Faculty of Dental Medicine, Hadassah Medical Center, 12000 Jerusalem, Israel;

^dGeneral Surgery Department, Hadassah Hebrew University Medical Center, 12000 Jerusalem, Israel; ^eDepartment of Immunology, Weizmann Institute of Science, 7610001 Rehovot, Israel; and ^fDepartment of Microbiology and Molecular Genetics, Faculty of Medicine, Hebrew University, 9190501 Jerusalem, Israel

Edited by Jason G. Cyster, University of California, San Francisco, CA, and approved December 26, 2018 (received for review November 2, 2018)

$\gamma\delta$ T cells are a major component of epithelial tissues and play a role in tissue homeostasis and host defense. $\gamma\delta$ T cells also reside in the gingiva, an oral tissue covered with specialized epithelium that continuously monitors the challenging dental biofilm. Whereas most research on intraepithelial $\gamma\delta$ T cells focuses on the skin and intestine epithelia, our knowledge on these cells in the gingiva is still incomplete. In this study, we demonstrate that even though the gingiva develops after birth, the majority of gingival $\gamma\delta$ T cells are fetal thymus-derived $V\gamma 6^+$ cells, and to a lesser extent $V\gamma 1^+$ and $V\gamma 4^+$ cells. Furthermore, we show that $\gamma\delta$ T cells are motile and locate preferentially in the epithelium adjacent to the biofilm. $V\gamma 6^+$ cells represent the major source of IL-17-producing cells in the gingiva. Chimeric mice and parabiosis experiments indicated that the main fraction of gingival $\gamma\delta$ T cells is radioresistant and tissue-resident, persisting locally independent of circulating $\gamma\delta$ T cells. Notably, gingival $\gamma\delta$ T cell homeostasis is regulated by the microbiota as the ratio of $V\gamma 6^+$ and $V\gamma 4^+$ cells was reversed in germ-free mice, and their activation state was decreased. As a consequence, conditional ablation of $\gamma\delta$ T cells results in elevated gingival inflammation and subsequent alterations of oral microbial diversity. Taken together, these findings suggest that oral mucosal homeostasis is shaped by reciprocal interplays between $\gamma\delta$ T cells and local microbiota.

oral mucosa | $\gamma\delta$ T cells | $V\gamma 6$ | microbiota | gingiva

The establishment of oral mucosal homeostasis is essential for human health (1, 2). Besides functioning as a physical barrier protecting the underlying tissues from microbial invasion and mechanical forces, the oral epithelium is known to have an immunological role. Oral epithelial cells are capable of producing antibacterial peptides and a variety of cytokines that regulate antimicrobial defense (3, 4). Gingival epithelial cells also produce IL-6 due to on-going damage from mastication, which drives homeostatic Th17 responses in the gingiva (5). Microbial colonization of the oral cavity was found to up-regulate expression of cytokines and chemokines that are considered to be involved in tissue homeostasis (6). Moreover, shortly after birth the microbiota induces the expression of growth arrest-specific protein 6 (GAS6) in the outermost layers of the oral epithelium; GAS6 in turn down-regulates the activation of epithelial cells and plays a critical role in the establishment of oral homeostasis (7). Besides epithelial cells, tissue-resident leukocytes colonize the oral epithelium and maintain immunological balance with the microbes on the other side of the epithelium. Langerhans cells (LCs), a special subset of antigen-presenting cells exclusively residing in stratified epithelia, were recently reported to regulate oral mucosal immunity and to prevent spontaneous alveolar bone loss (8, 9). Thus, both hematopoietic and nonhematopoietic cells that constitute the epithelium are shaping homeostasis in the oral mucosa.

$\gamma\delta$ T cells are innate T lymphocytes residing in high abundance in epithelial surfaces, including the oral epithelium (10, 11). This

is reminiscent of the skin and intestine, where intraepithelial $\gamma\delta$ T cells represent the majority of epithelial T cells and were shown to function as local sentinels (12). $\gamma\delta$ T cells can be divided into different subgroups based on the V-segment they express in the variable region of the T cell receptor (TCR) γ -chain. These subgroups are differentially localized among tissues, secrete distinct cytokines, and develop at different periods in the thymus (13, 14). While $V\gamma 1^+$ and $V\gamma 4^+$ $\gamma\delta$ T cells arise from both embryonic and adult thymus, $V\gamma 5^+$ and $V\gamma 6^+$ $\gamma\delta$ T cells develop as natural effector T cells only in the embryonic thymus and display a restricted TCR repertoire (15, 16). Because of their pre-activated effector phenotype and highly specific tissue residence, $\gamma\delta$ T cells can rapidly respond to perturbations in mucosal tissue integrity and homeostasis (14). Studies suggested that $\gamma\delta$ T cells could directly recognize microbial antigen and respond by production of effector cytokines, such as IL-17A (17, 18). Intraepithelial $\gamma\delta$ T cells can also limit transepithelial pathogen invasion and contribute to immune protection in mucosal tissues (19). On the other hand, $\gamma\delta$ T cells can enhance the pathogenesis of inflammatory diseases, such as psoriasis-like dermatitis and spondyloarthritis (20, 21).

Significance

Elucidating the mechanisms by which homeostasis is established and maintained in the oral mucosa is important for human health. In this study we investigated the ontogeny and function of gingival $\gamma\delta$ T cells. The majority of these cells originate from embryonic precursors that maintain themselves locally independent of circulating $\gamma\delta$ T cells arising from adult precursors. The oral microbiota regulates the development of $\gamma\delta$ T cells, particularly those of embryonic origin. $\gamma\delta$ T cells represent the major sources of IL-17-producing cells in the gingiva, and they play a critical role in down-modulating gingival steady-state immunity that subsequently shapes oral microbial diversity. This suggests that oral homeostasis requires mutual interactions between $\gamma\delta$ T cells and the microbiota.

Author contributions: A. Wilensky, R.F., H.B., I.P., and A.-H.H. designed research; A. Wilharm, Y.T., M.N., A.R., G.M., I.S., J.B.-M., Y.A., A.K., and L.E.-B. performed research; E.E. contributed new reagents/analytic tools; A. Wilharm, Y.T., I.S., O.H., Y.A., and R.F. analyzed data; and I.P. and A.-H.H. wrote the paper.

The authors declare no conflict of interest.

This article is a PNAS Direct Submission.

Published under the PNAS license.

¹A. Wilharm and Y.T. contributed equally to this work.

²Present address: Division of Immunology and Allergy, Department of Medicine Solna, Karolinska Institutet, Karolinska University Hospital Solna, 171 76 Stockholm, Sweden.

³I.P. and A.-H.H. contributed equally to this work.

⁴To whom correspondence may be addressed. Email: prinz.immo@mh-hannover.de or avihaih@ekmd.huji.ac.il.

This article contains supporting information online at www.pnas.org/lookup/suppl/doi:10.1073/pnas.1818812116/-DCSupplemental.

Whereas the aforementioned observations highlight the immunological function of intraepithelial $\gamma\delta$ T cells, most research on these cells focused on the skin and intestinal epithelium, while our knowledge on $\gamma\delta$ T cells in the oral epithelium is incomplete. The oral epithelium shares many features with epithelia of the skin and intestine, yet has its own distinctive characteristics. On a structural aspect, the oral mucosa possesses a stratified squamous epithelium similar to the epidermis and not a single-layer epithelium that covers the intestine. However, whereas the epidermis is not accessible to cells from the circulation at steady state, the oral epithelium, akin to the intestine, is constantly replenished by circulating leukocytes (9). The oral mucosa also deals with a unique microbial challenge, the persistent dental biofilm, where the gingival epithelium serves as a protective barrier that monitors it (1). Therefore, immune surveillance in the gingiva is complex and homeostasis is often disrupted, resulting in both oral and systemic medical pathologies (2). Thus, understanding the role of $\gamma\delta$ T cells in gingival homeostasis is an important task. Furthermore, because the gingiva is created only after birth (i.e., simultaneously with tooth eruption), the contribution of embryonic- versus adult-derived $\gamma\delta$ T cells to the overall gingival $\gamma\delta$ T cell population is intriguing. This study investigated the development and steady-state function of gingival $\gamma\delta$ T cells in correlation to the oral microbiota.

Results

Intraepithelial $\gamma\delta$ T Cells of the Gingiva Are Motile and Localize Close to the Biofilm. The stratified gingival epithelium can be divided into three sections: the junctional epithelium that is attached to the tooth surface, the sulcular epithelium lining the gingival sulcus, and the oral epithelium covering the external surface of the gingiva. To visualize the distribution of intraepithelial $\gamma\delta$ T cells in the various specialized gingival epithelia, we performed immunofluorescence microscopy on gingival cross-sections of *TcrdH2BeGFP* reporter mice expressing the GFP in the nuclei of $\gamma\delta$ T cells. As demonstrated in Fig. 1A and B, $\gamma\delta$ T cells were mainly located in the junctional epithelium in close proximity to the dental biofilm. Furthermore, whereas $\gamma\delta$ T cells in the oral and sulcular epithelium mostly reside in the basal layers of the epithelium, they were also detected in suprabasal layers of the junctional epithelium. $\gamma\delta$ T cells were also observed in the lamina propria underlying the epithelium, and most of the cells were positioned close to the basal membrane. By whole-mount immunofluorescence microscopy staining on gingival epithelial sheets, we detected round-shaped CD3⁺ $\gamma\delta$ T cells close to the epithelial margin (Fig. 1C). In contrast, $\gamma\delta$ T cells in the skin epidermis were evenly distributed and had a characteristic dendritic-like shape (22) (SI Appendix, Fig. S14). We next applied *in vivo* two-photon laser-scanning microscopy on gingival tissues of the incisors using narcotized *TcrdH2BeGFP* mice. The large majority of $\gamma\delta$ T cells were localized in the gingival epithelium above the second harmonic signal, which was generated by collagen structures of the connective tissue (Fig. 1D). This setting also identified $\gamma\delta$ T cells within the connective tissue, as GFP⁺ cells were detected very close to the second harmonic signal. Importantly, two-photon laser-scanning *in vivo* microscopy analysis revealed that most gingival intraepithelial $\gamma\delta$ T cells were motile (Movie S1), and thus permanently screening their tissue of residency. We next performed flow cytometric analysis of $\gamma\delta$ T cells in the gingival epithelium and lamina propria. Because the gingival epithelium and its connective tissue structurally resemble the skin epidermis and dermis, we compared gingival $\gamma\delta$ T cells to those residing in the skin. Consistent with previous findings, langerin/CD207⁺ cells were exclusively located in both epithelia (9). Concurring with the histology results, $\gamma\delta$ T cells were found in both the epithelium and lamina propria of the gingiva similar to the skin compartments (Fig. 1E). Nevertheless, TCR expression levels on intraepithelial $\gamma\delta$ T cells were lower in the gingiva in comparison with the skin epidermis. Next, we found that in contrast to the epidermis in which $\gamma\delta$ T cells represent the dominating T cell subset, intraepithelial gingival $\gamma\delta$ T cells represented about

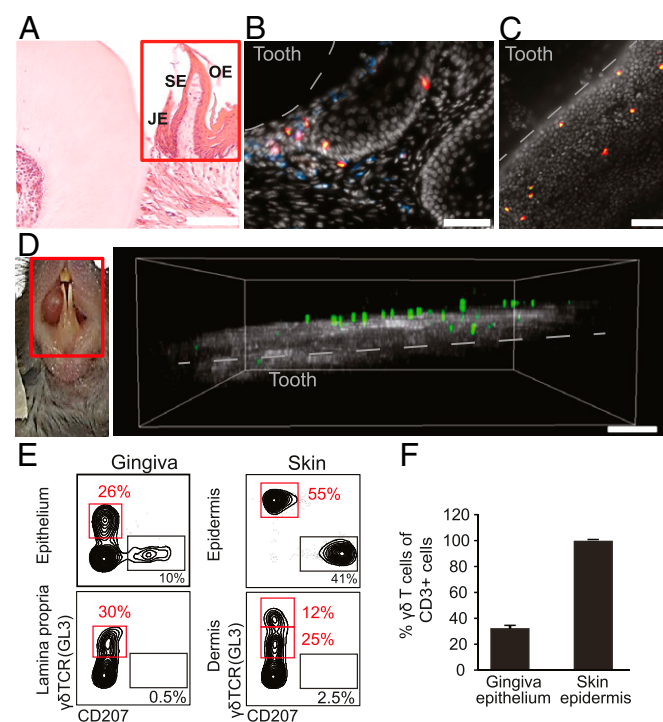


Fig. 1. Visualization of $\gamma\delta$ T cells in the oral mucosa. (A) H&E histological staining of cross sections of the maxilla of adult *TcrdH2BeGFP* mice. The red rectangle specifies the gingival mucosa. JE, junctional epithelium; OE, oral epithelium; SE, sulcular epithelium. One representative of three independent analyses. (Scale bar, 100 μ m.) (B) Immunofluorescence staining of cross sections of the maxilla of adult *TcrdH2BeGFP* mice ($\gamma\delta$ T cells in green/eGFP) with mAbs directed against CD45 (blue), CD3 (red), and with DAPI (white) for nuclear visualization. Representative image of four independent experiments. (Scale bar, 50 μ m.) (C) Immunofluorescence whole mount staining from gingival epithelial layers of adult *TcrdH2BeGFP* mice with mAbs directed against CD3 (red) and with DAPI (white). Representative image from four independent experiments. Dotted white line indicates the location of the tooth surface. (Scale bar, 50 μ m.) (D) Two-photon microscopy on gingival tissues of the lower incisors (Left; red rectangle indicates imaging area) of adult *TcrdH2BeGFP* mice demonstrating the localization of $\gamma\delta$ T cells (green/eGFP) close to collagen structures (gray) (Right). Representative image of three independent experiments. (Scale bar, 70 μ m.) (E and F) Epithelial and lamina propria/dermal layers were prepared from the gingiva or skin, and stained with antibodies against CD45, $\gamma\delta$ TCR, and langerin. (E) Representative FACS plots present the frequencies of $\gamma\delta$ T cells in each tissue. (F) Bar graphs depict percentages of $\gamma\delta$ T cells among total CD3⁺ cells in the gingiva and skin epithelium ($n = 3$). Data are representative of four independent experiments.

30% of the T cell population (Fig. 1F). Taken together, these data indicate that the gingiva contains a clear population of intraepithelial $\gamma\delta$ T cells that is morphologically and quantitatively different from skin epidermal $\gamma\delta$ T cells. Moreover, gingival intraepithelial $\gamma\delta$ T cells are motile and reside predominantly in the junctional epithelium, suggesting a role for these cells in steady-state monitoring of the oral biofilm.

Gingival $\gamma\delta$ T Cells Have an Activated IL-17-Secreting Phenotype. We next sought to characterize the effector phenotype and activation status of gingival $\gamma\delta$ T cells using flow cytometry. First, we analyzed $\gamma\delta$ T cell subsets in the gingiva based on their V-segment expression in the TCR γ -chain. Of total gingival $\gamma\delta$ T cells in adult mice, $63 \pm 2.3\%$ were $V\gamma 6^+$ (Fig. 2A) and were localized in the epithelium as well as the lamina propria (SI Appendix, Fig. S2A). Other subsets included $V\gamma 1^+$ ($17.3 \pm 2.6\%$), $V\gamma 4^+$ ($7.3 \pm 1\%$), $V\gamma 5^+$ ($6.5 \pm 1.1\%$), and $V\gamma 7^+$ ($3.2 \pm 0.8\%$) $\gamma\delta$ T cells, taken together representing $>97\%$ of gingival $\gamma\delta$ T cells (Fig. 2A). In comparison, the main subsets in peripheral lymph nodes were

$V\gamma 1^+$ and $V\gamma 4^+$ $\gamma\delta$ T cells, while $V\gamma 6^+$ $\gamma\delta$ T cells only represented a minor population (SI Appendix, Fig. S2B). Next, we examined the expression of activation markers on gingival intraepithelial $\gamma\delta$ T cells compared with epidermal $\gamma\delta$ T cells. Elevated expression of CD44 and CD69 combined with the lack or low expression of CD62L and CD24 indicated an activated phenotype of intraepithelial as well as lamina propria $\gamma\delta$ T cells in the gingiva (Fig. 2B and SI Appendix, Fig. S2C).

Further phenotypic analysis demonstrated that CD25 (IL-2 receptor- α chain) was slightly up-regulated on intraepithelial $\gamma\delta$ T cells of the gingiva compared with the epidermis, whereas expression of CD122 (IL-2 receptor- β chain) was not altered. Expression of the CD103 integrin was elevated on intraepithelial $\gamma\delta$ T cells in both the gingiva and skin (SI Appendix, Fig. S2C). Next, intracellular cytokine staining revealed that $50.6 \pm 5.3\%$ of

gingival effector $\gamma\delta$ T cells produced IL-17 and only $5.6 \pm 2.6\%$ secreted IFN- γ after ex vivo stimulation (Fig. 2C). Furthermore, $V\gamma 6^+$ $\gamma\delta$ T cells were the predominant IL-17-producing cells (SI Appendix, Fig. S2D). Concurring with this cytokine profile, the majority of gingival $\gamma\delta$ T cells showed a typical $\gamma\delta$ T17 phenotype ($CD27^-, NK1.1^- CD44^{hi}$) (SI Appendix, Fig. S2F). Gating on IL-17 production among all gingival CD45 $^+$ leukocytes demonstrated that $\gamma\delta$ T cells are the main source of IL-17 in the gingiva ($70.7 \pm 3.5\%$ of IL-17-expressing cells) (Fig. 2D). Because we observed that $\gamma\delta$ T cells secrete IL-17 after ex vivo stimulation, we asked whether these cells would produce this proinflammatory cytokine in vivo within the gingiva of *Il17eGFP* reporter mice. Similar to ex vivo stimulation, 60% of $\gamma\delta$ T cells in the gingiva of *Il17eGFP* mice were $CD44^{hi}$ and GFP $^+$, indicative of in vivo IL-17 secretion at steady state, whereas $\alpha\beta$ T cells barely produced

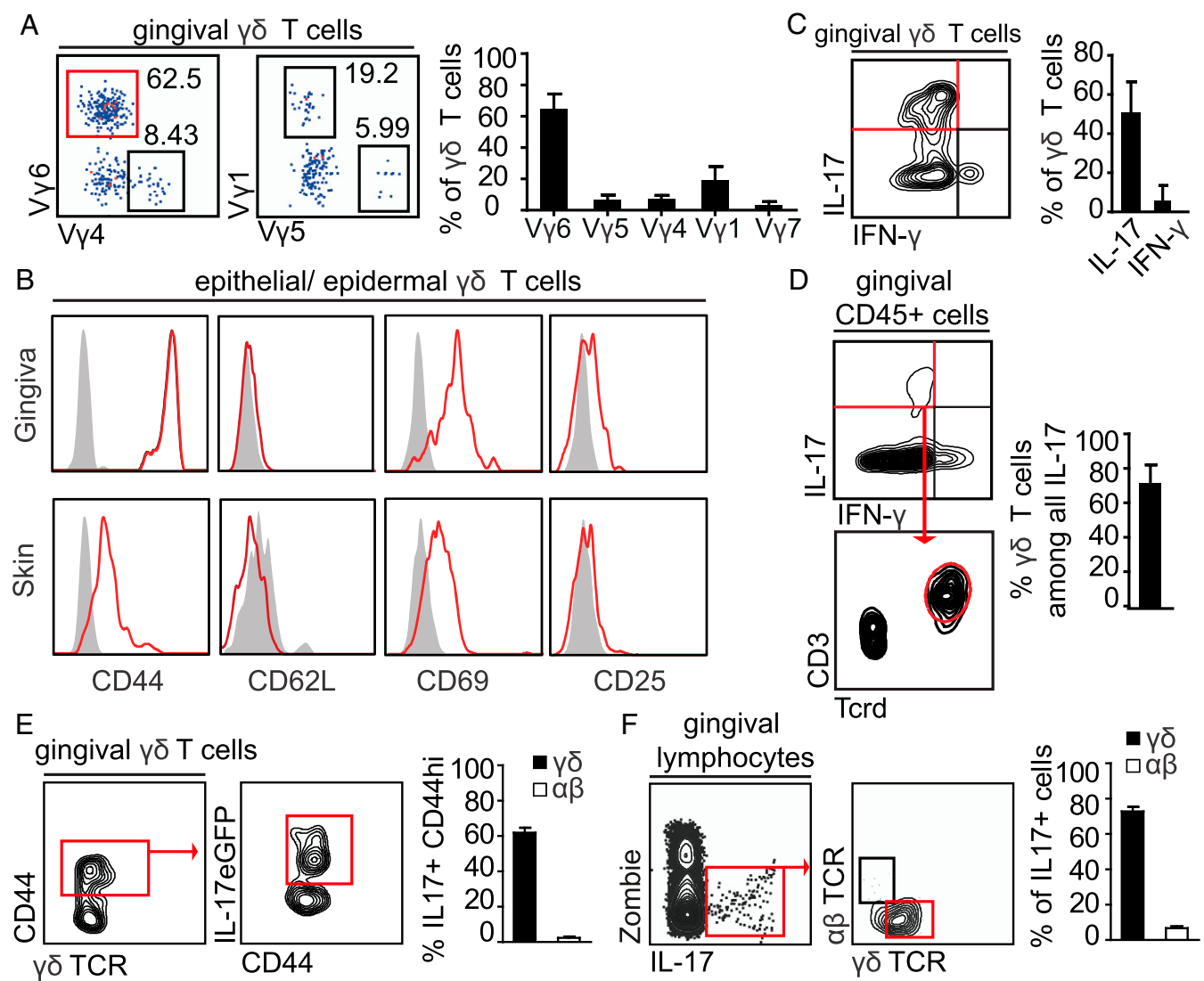


Fig. 2. Characterization of $\gamma\delta$ T cells in the oral mucosa. (A) FACS plots show γ -chain usage by gingival $\gamma\delta$ T cells from adult *TcrdH2BeGFP* mice. Bar graphs depict mean frequencies + SEM of γ -chain types of gingival $\gamma\delta$ T cells. Data are pooled from two to three independent experiments ($n = 3$ –7 mice per experiment). (B) Expression of selected typical surface markers on $\gamma\delta$ T cells in the gingiva and skin epithelium. Gray filled histograms represent isotype controls (Ctl). Data representative of three independent experiments ($n = 5$ mice in each experiment). (C and D) Isolated gingival lymphocytes were stimulated ex vivo with phorbol myristate acetate (PMA) and ionomycin. Representative FACS plots of three independent experiments ($n = 3$ –4 mice per experiment). Bar graphs present the mean frequencies + SEM of pooled data from six experiments. FACS plots and bar graphs show $\gamma\delta$ T cells expressing IL-17 or IFN- γ and the relative contribution of $\gamma\delta$ T cells to IL-17-expressing total leukocytes in the tissue. (E and F) IL-17 production analyzed directly ex vivo in gingival $\gamma\delta$ T cells from *Il17eGFP* reporter mice. (E) IL-17 $^+$ cells among $CD44^{hi}$ $\gamma\delta$ T cells. Bar graph depicts means + SEM of pooled frequencies from two independent experiments ($n = 4$ mice per experiment). (F) Frequencies of $\gamma\delta$ T cells and $\alpha\beta$ T cells among all IL-17 $^+$ cells in the gingival tissue, two independent experiments ($n = 4$ mice per experiment). Bar graph shows mean frequency + SEM of pooled data from two independent experiments.

IL-17 (~2% of CD44^{hi} $\alpha\beta$ T cells) (Fig. 2E). After gating on all IL-17⁺ cells in the gingiva, $\gamma\delta$ T cells represented the main subset of IL-17-producing cells in this setting (Fig. 2F). In contrast to the gingiva, merely 12.8% among CD44^{hi} $\gamma\delta$ T cells in peripheral lymph nodes produced IL-17 in *IL17eGFP* mice (*SI Appendix*, Fig. S2F). However, the IL-17 secretion level in lymph nodes was nearly tripled (33.6 \pm 3.8%) when the cells were stimulated ex vivo (*SI Appendix*, Fig. S2G). To sum up, the large majority of gingival $\gamma\delta$ T cells expresses V γ 6 and has a preactivated phenotype representing the main IL-17-producing lymphocyte subset in this oral tissue.

Gingival $\gamma\delta$ T Cells Are Partially Dependent on CCR6 and IL-23R Signaling

Signaling. IL-23 signaling has been suggested to be crucial for the development and maintenance of IL-17-producing $\alpha\beta$ T cells (23, 24). Hence, we asked whether IL-23 receptor (IL-23R) signaling is also required for the maintenance and proliferation of gingival $\gamma\delta$ T cells. Using heterozygous *Il23r^{gfp/+}* knockin mice, we found that IL-23R-expressing $\gamma\delta$ T cells were almost exclusively V γ 6⁺ T cells (*SI Appendix*, Fig. S3A). In *Il23r^{gfp/gfp}* mice lacking IL-23R, we observed a significantly reduced number of $\gamma\delta$ T cells in the gingiva while $\alpha\beta$ T cells were not affected, concurring with our earlier observations that gingival $\alpha\beta$ T cells are not IL-17 producers (*SI Appendix*, Fig. S3B). In particular, V γ 6⁺ T cells expressing IL-23R were dramatically reduced but not absent in the gingiva of *Il23r^{gfp/gfp}* mice lacking IL-23R signaling (*SI Appendix*, Fig. S3C). Next, we investigated whether the chemokine receptors, CCR6 and CX₃CR1, played a role in the homing of gingival $\gamma\delta$ T17 cells, as suggested for other tissues (25–28). To this end, we used CX₃CR1 and CCR6 GFP knockin transgenic mice. As demonstrated in *SI Appendix*, Fig. S3D, epidermal $\gamma\delta$ T cells homogenously expressed CX₃CR1. In contrast, only 18% of the $\gamma\delta$ T cells in the gingival epithelium expressed CX₃CR1. However, deletion of the receptor CX₃CR1 in *Cx3cr1^{gfp/gfp}* mice had no impact on the frequencies of $\gamma\delta$ T cells in the gingival epithelium, as well as in the skin epidermis (*SI Appendix*, Fig. S3E). As for CCR6, while no $\gamma\delta$ T cells in the epidermis express this receptor, nearly 25% of gingival $\gamma\delta$ T cells expressed CCR6 (*SI Appendix*, Fig. S3F). The absence of CCR6 in *Ccr6^{gfp/gfp}* mice led to a significant reduction in intraepithelial $\gamma\delta$ T cells in the gingiva, but not in skin (*SI Appendix*, Fig. S3G). In conclusion, the homeostasis of V γ 6⁺ T cells in the gingiva is partially dependent on IL-23R signaling, while CCR6 drives homing of part of the $\gamma\delta$ T cells to the gingival epithelium.

$\gamma\delta$ T Cells Reside in the Prospective Gingival Epithelium During Embryogenesis and Their Numbers Increase Postnatally but Decline with Age. The gingiva is a special tissue because it emerges postnatally during the process of tooth eruption, starting in mice during the second week after birth. To track the development of gingival intraepithelial $\gamma\delta$ T cells, we first collected the epithelium of the prospective gingiva at postnatal day (P)7, as well as during gingiva development at days P10 and P13. A small population of intraepithelial $\gamma\delta$ T cells was detectable at P7 and the frequency of these cells increased relatively fast in the epithelium later on (Fig. 3A). In fact, the frequencies of $\gamma\delta$ T cells on P13 were similar to those observed in adult mice (~25–30% of total leukocytes in the epithelium). In contrast to the gingiva, $\gamma\delta$ T cells in the epidermis were established already at day P7. Because V γ 6⁺ $\gamma\delta$ T17 cells might have entered the oral mucosa already during embryogenesis, we examined $\gamma\delta$ T cells in the tongue, an oral tissue that is accessible for analysis at embryonic day (E)14.5. Indeed, a clear population of CD3⁺ $\gamma\delta$ T cells was observed in the tongue mucosa at this early developmental stage (Fig. 3B). A small population of $\gamma\delta$ T cells was also found in the limb bud representing the developing skin (Fig. 3B).

To investigate whether gingival $\gamma\delta$ T cells develop in embryonic thymus or arise from postnatal development, we used the *Indu-Rag1* \times *TcrdH2BeGFP* mice (29). These mice lack B and T lymphocytes due to the absence of recombination-activating gene 1

(*Rag1*), but maturation of B and T cells can be initiated in adult mice upon administration of tamoxifen. Seven weeks after tamoxifen treatment, *Indu-Rag1* \times *TcrdH2BeGFP* mice had reduced frequencies of $\gamma\delta$ T cells in the gingiva (Fig. 3C), whereas $\alpha\beta$ T cells were completely restored (*SI Appendix*, Fig. S4A). Furthermore, V γ 6⁺ $\gamma\delta$ T cells were completely absent in these mice, confirming that their development is restricted to the embryonic thymus (Fig. 3D). Interestingly, $\gamma\delta$ T cells present in the gingiva of tamoxifen-treated *Indu-Rag1* \times *TcrdH2BeGFP* adult

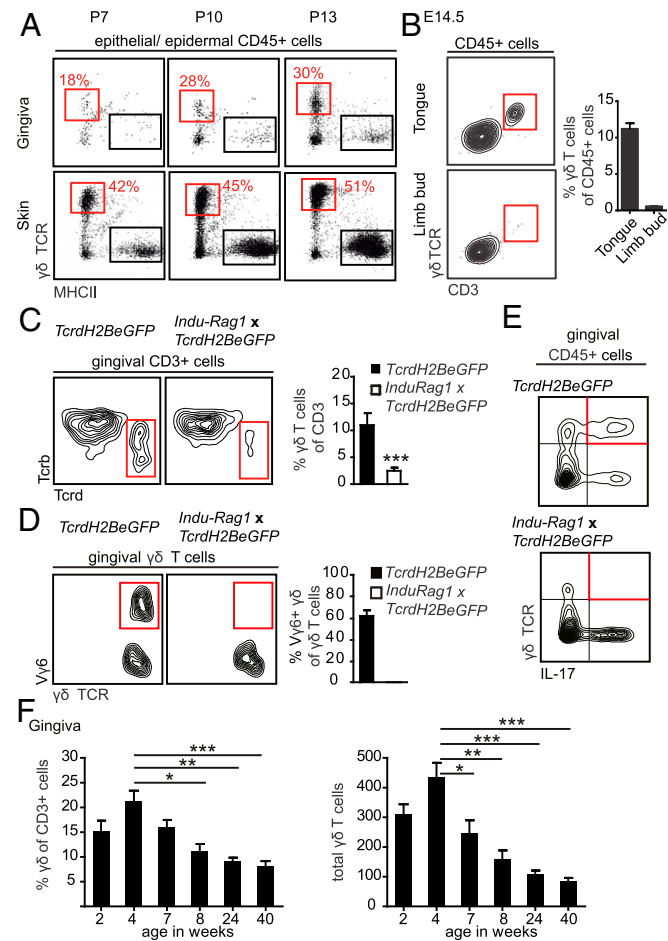


Fig. 3. Oral $\gamma\delta$ T cells develop prenatally, expand postnatally, but decline with age. (A) FACS plots show frequencies of epithelial $\gamma\delta$ T cells in the gingiva and skin at indicated days postnatally (P). Five to six mice were analyzed in each experiment, two independent experiments. (B) Representative FACS plots and bar graph demonstrating the presence of $\gamma\delta$ T cells in the tongue and limb buds on day E14.5 (three independent experiments; eight embryos were analyzed in each experiment). (C) $\gamma\delta$ T cell populations among CD3⁺ cells in gingival tissues form *TcrdH2BeGFP* and *Indu-Rag1* \times *TcrdH2BeGFP* adult mice. Representative FACS plots from three independent experiments. Bar graph depicts the mean frequencies \pm SEM of $\gamma\delta$ T cells among total gingival CD3⁺ T cells. (Data pooled from three independent experiments, $n = 7$ –8 mice per experiment.) (D) Frequencies of V γ 6⁺ cells from total gingival $\gamma\delta$ T cells of *TcrdH2BeGFP* and *Indu-Rag1* \times *TcrdH2BeGFP* mice. Bar graph demonstrates mean frequencies \pm SEM of V γ 6⁺ cells among total gingival $\gamma\delta$ T cells. Data were pooled from two independent experiments ($n = 8$ mice per experiment). (E) FACS plots show $\gamma\delta$ T cells producing IL-17 from total gingival leukocytes isolated from *TcrdH2BeGFP* and *Indu-Rag1* \times *TcrdH2BeGFP* mice and stimulated ex vivo with PMA and ionomycin. (Three independent experiments, $n = 8$ –10 mice per experiment.) (F) Frequencies and total numbers of murine gingival $\gamma\delta$ T cells throughout life. Data pooled from three independent experiments are shown and presented as the mean values \pm SEM ($n = 6$ –9 mice per experiment). * $P < 0.05$, ** $P < 0.01$, *** $P < 0.001$.

mice failed to produce IL-17 upon ex vivo stimulation, but this task was taken over by other non- $\gamma\delta$ T lymphocytes in the gingiva (Fig. 3E). Next, we examined the frequencies of gingival $\gamma\delta$ T cells throughout life, because age is known to have a major impact on oral homeostasis (30). Whereas frequencies and absolute numbers of $\gamma\delta$ T cells increased in the gingiva during the first 4 wk after birth, a sharp and significant reduction was observed in 8-wk-old mice (Fig. 3F). The frequency and numbers of $\gamma\delta$ T cells gradually declined afterward, and in 40-wk-old mice gingival $\gamma\delta$ T cells were reduced three- to fourfold in comparison with 4-wk-old mice (Fig. 3F). Accordingly, total numbers of $V\gamma 6^+$ cells declined in 40-wk-old mice compared with 4-wk-old mice (SI Appendix, Fig. S4B). However, the frequencies of these cells among all $\gamma\delta$ T cells were not altered, which suggests that non- $V\gamma 6^+$ cells were also reduced with age. Analysis of gingival intraepithelial $\gamma\delta$ T cells in aged (18-mo-old) mice showed a significant reduction in their frequencies compared with 2-mo-old adult mice (SI Appendix, Fig. S4C). In contrast, the frequency of epidermal $\gamma\delta$ T cells was not decreased in aged mice. In conclusion, $\gamma\delta$ T cells, predominantly $V\gamma 6^+$ cells, enter the oral epithelium during embryogenesis and increase during weaning until 4 wk of age. Later, aging is accompanied with a gradual loss of $\gamma\delta$ T cells.

Gingival Intraepithelial $\gamma\delta$ T Cells Comprise Radioresistant and Tissue-Resident Populations. To investigate the homeostasis and turnover of gingival $\gamma\delta$ T cells, we first evaluated the kinetics of these cells following continuous administration of BrdU. Seven days after BrdU treatment, about 30% of the intraepithelial $\gamma\delta$ T cells were BrdU⁺ and levels doubled after 14 d of treatment (SI Appendix, Fig. S5). In contrast, epidermal $\gamma\delta$ T cells showed only negligible BrdU-labeling levels (SI Appendix, Fig. S5). Next, we reconstituted lethally irradiated CD45.2⁺ B6 mice with bone marrow

purified from congenic CD45.1⁺ mice. Two weeks after irradiation, a significant decrease in the frequencies of gingival intraepithelial $\gamma\delta$ T cells was detected, which was further reduced 8-wk postirradiation (Fig. 4A). The population of $\gamma\delta$ T cells then slowly expanded in the gingival epithelium, reaching about half of the original frequencies 12 mo after the irradiation. Importantly, the majority of reconstituting $\gamma\delta$ T cells (~58%) developed from the host, whereas donor-derived $\gamma\delta$ T cells constituted only 38% of the population (Fig. 4A). Thus, gingival intraepithelial $\gamma\delta$ T cells contain a radioresistant population and an additional population arriving via the circulation. To directly examine the origin of intraepithelial $\gamma\delta$ T cells, we generated parabiotic mice by pairing surgically CD45.2⁺ B6 mice with congenic CD45.1⁺ mice, so the mice shared the same blood circulation but had separate organs. Two weeks after parabiosis ~10% of the $\gamma\delta$ T cells originated from circulating cells, while their frequencies increased to 20–30% after 6 wk (Fig. 4B). Because in parabiotic mice the circulating leukocytes from both parabionts are evenly divided, the contribution of circulating cells to intraepithelial $\gamma\delta$ T cells in this setting was in fact 40–60%. As an expected control for the parabiosis experiments, no contribution from the circulation was found in epidermal $\gamma\delta$ T cells. Taken together, these data thus suggest that gingival intraepithelial $\gamma\delta$ T cells contain a population of tissue-resident and radioresistant cells with self-renewing capability. An additional population comprising approximately half of the intraepithelial $\gamma\delta$ T cells originated from the circulation, and replaced constitutively and independently of the tissue-resident population.

The Microbiota Regulates the Frequency, $V\gamma$ Chain Subset Composition, and Activation of Gingival $\gamma\delta$ T Cells. The localization of intraepithelial $\gamma\delta$ T cells in the junctional epithelium, as well as their expansion after birth, suggest an interplay with the microbiota.

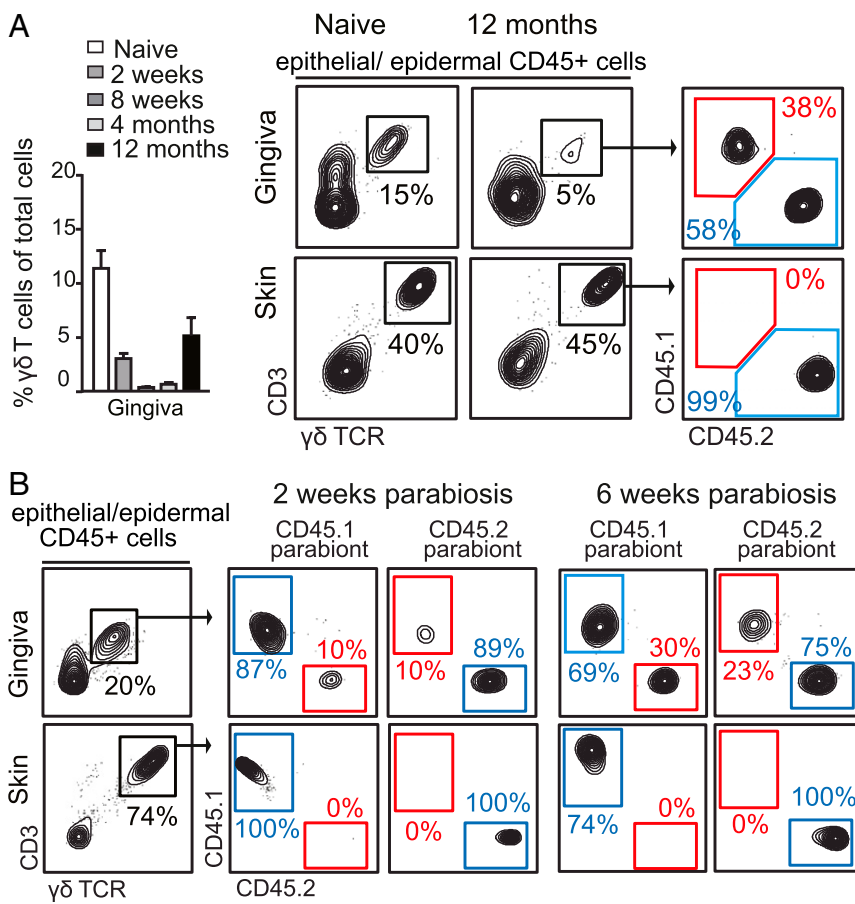


Fig. 4. Oral $\gamma\delta$ T cells comprise both radioresistant tissue-resident cells and radiosensitive circulating cells. (A) Lethally irradiated CD45.2⁺ B6 mice were transplanted with bone marrow purified from congenic CD45.1⁺ B6 mice. Representative FACS plots demonstrate the contribution of donor (CD45.1⁺ cells) to $\gamma\delta$ T cells in the gingiva and skin epithelium 12 mo after the transplantation. Bar graphs depict the frequencies of $\gamma\delta$ T cells in the gingival epithelium at various times after the bone marrow transplantation ($n = 4$ –6 mice per group for each time point). FACS plots represent the results of one of two independent experiments with similar results, and graphs present the mean values \pm SEM. (B) CD45.1⁺ B6 and CD45.2⁺ B6 mice were joined surgically for the generation of parabiotic pairs, and homeostasis of $\gamma\delta$ T cells was analyzed 2 and 6 wk after parabiosis in each parabiont. Representative flow cytometry plots from four independent experiments ($n = 3$ –4 pairs per time point).

To examine this issue directly, we analyzed $\gamma\delta$ T cells in adult germ-free (GF) mice. The absence of the microbiota resulted in decreased frequencies and total numbers of gingival $\gamma\delta$ T cells (Fig. 5A and *SI Appendix*, Fig. S6A) but not of skin intraepithelial $\gamma\delta$ T cells (Fig. 5B). In contrast, the frequencies of $\alpha\beta$ T cells were elevated in the gingiva of GF mice compared with specific pathogen-free (SPF) mice (*SI Appendix*, Fig. S6B). Moreover, among the $\gamma\delta$ T cells, the frequency and number of the $V\gamma 6^+$ subset was greatly reduced, whereas the relative frequencies but not the numbers of $V\gamma 4^+$ T cells were elevated (Fig. 5C and *SI Appendix*, Fig. S6A). Further analysis revealed that the frequencies as well as total numbers of $CD44^{hi}$ $\gamma\delta$ T cells were reduced in the gingiva of GF mice in comparison with SPF mice, suggesting a lower activation state of these cells in the absence of the oral microbiota (Fig. 5D and *SI Appendix*, Fig. S6A). The activation status of conventional $\alpha\beta$ T cells in the gingiva was not significantly reduced (*SI Appendix*, Fig. S6B). Concurring with the reduction in $V\gamma 6^+$ and $CD44^{hi}$ $\gamma\delta$ T cells found in GF mice, IL-17 levels were reduced in the gingiva of these mice compared with the SPF group (Fig. 5E). Interestingly, in GF mice we did not observe a reduction in frequencies or activation status of total $\gamma\delta$ T cells in cervical lymph nodes that drain the oral mucosa (*SI Appendix*, Fig. S6C). Nevertheless, the frequency of the $V\gamma 6^+$ subset was significantly reduced, whereas at the same time the proportion of $V\gamma 4^+$ T cells increased in the mucosa-draining lymph nodes of GF mice (*SI Appendix*, Fig. S6C). To examine whether $\gamma\delta$ T cells are also responsive to changes in the microbiota in an adult host after the establishment of the microbiota, we next treated adult B6 mice with broad-spectrum antibiotic in the drinking water for 2 mo. A significant reduction in the frequency of intraepithelial $\gamma\delta$ T cells was detected in the gingiva but not epidermis of antibiotic-treated mice in comparison with the untreated control group (Fig. 5F). Taken together, these findings suggest that development and function of gingival $\gamma\delta$ T cells is critically regulated by the microbiota. Moreover, gingival $V\gamma 6^+$ T cells appeared to be most responsive to the oral microbiota.

Conditional Ablation of $\gamma\delta$ T Cells Elevates the Inflammatory Milieu in the Gingiva. We next addressed whether $\gamma\delta$ T cells play a role in the maintenance of immunological homeostasis in the oral mucosa. To this end, we used the *Tcrd-GDL* knockin mice, which express simultaneously three reporter genes (GDL; *Gfp-Dtr-Luc*) specifically expressed in $\gamma\delta$ T cells under the control of successfully rearranged TCR δ genes. The expression of diphtheria toxin (DT) receptor in *Tcrd-GDL* mice allows the depletion in vivo of $\gamma\delta$ T cells upon administration of DT. First, we examined the repopulation kinetics of $\gamma\delta$ T cells upon a single administration of DT to adult *Tcrd-GDL* mice. Depletion of gingival intraepithelial $\gamma\delta$ T cells was evident 24 h after DT treatment (Fig. 6A). In the following weeks, the $\gamma\delta$ T cells gradually reappeared in the gingival epithelium, but failed to reach their original frequencies as far as 8 wk after DT treatment. We also analyzed the repopulation of $\gamma\delta$ T cells in the whole gingiva while focusing on the $V\gamma 6^+$ T cell subset. Similar slow repopulation kinetics were detected for total gingival $\gamma\delta$ T cells; nevertheless, the repopulating cells appeared to be non- $V\gamma 6^+$ cells (Fig. 6B). Next, to elucidate the impact of $\gamma\delta$ T cell ablation on oral immunity, we depleted these cells for 5 mo by injecting mice with DT on a weekly basis. Of note, we previously reported that such prolonged administration of DT into wild-type mice had no impact on gingival immunity and associated pathologies (8, 31). *Tcrd-GDL* mice receiving the PBS vehicle were used as a negative control. Flow cytometry analysis of gingival tissues isolated from long-term depleted mice revealed major changes in innate leukocytes. Specifically, the frequencies of neutrophils and monocytes were increased in DT-treated mice (Fig. 6C). Whereas the levels of total $CD4^+$ T cells and B cells were not altered by the DT treatment, higher levels of FOXP3-expressing $CD4^+$ T cells (T regulatory cells) were found in DT-treated mice compared with control group (Fig. 6C).

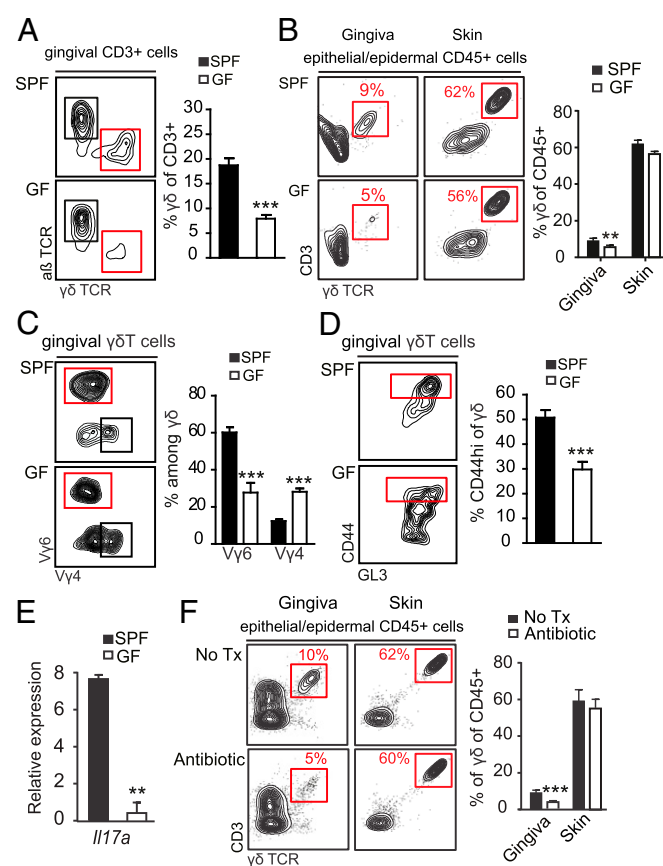


Fig. 5. Commensal microbiota regulate the development and activation state of oral $\gamma\delta$ T cells. Gingival tissues were collected and processed from adult SPF and GF mice for flow cytometry analysis. (A) FACS plots and graphs depict the frequencies of $\gamma\delta$ T cells in the whole gingiva. Data are representative of four independent experiments. Bar graphs present the mean values + SEM of pooled data from four independent experiments ($n = 7$ –10 mice per experiment). (B) Epithelial tissues were collected from the gingiva and skin of SPF and GF B6 mice. Representative FACS plots show the frequencies of $\gamma\delta$ T cells in each tissue. Bar graph presents the percentages of $\gamma\delta$ T cells among $CD45^+$ cells as the mean values + SEM ($n = 4$ mice, three independent experiments). (C) Percentages of $V\gamma 6^+$ and $V\gamma 4^+$ $\gamma\delta$ T cells and (D) levels of $CD44^{hi}$ $\gamma\delta$ T cells in the gingiva of GF and SPF mice. FACS plots are representative of four independent experiments. Bar graphs present the mean values + SEM of pooled data from four independent experiments ($n = 7$ –10 mice per experiment). (E) Expression of *IL17a* mRNA in the gingiva of GF or SPF mice. Results of one of two independent experiments are shown as the mean values + SEM ($n = 5$ mice per group). (F) Adult SPF B6 mice were treated with a broad-spectrum antibiotic mixture in the drinking water for 2 mo. Representative FACS plots and graph demonstrate the percentages of $\gamma\delta$ T cells in gingival and ear skin epithelial tissues of antibiotic-treated mice and control group ($n = 5$). Results of two independent experiments are shown as the mean values + SEM. * $P < 0.05$, ** $P < 0.01$, *** $P < 0.001$.

We next quantified in the gingiva the expression of certain gene groups using qRT-PCR. As demonstrated in Fig. 6D, mRNA levels of the ligand *Gas6* but not its receptor *Axl* were reduced in DT-treated mice in comparison with control mice. We recently showed that GAS6/AXL signaling down-regulates IFN I signaling (IFN- α/β) in the gingival epithelium, which is crucial for oral homeostasis (7). In line with this view, DT-treated mice expressed significantly higher levels of *Ifna* and *Ifnb* mRNA (Fig. 6D). We further quantified the mRNA levels of inflammation-associated cytokines such as *Ifng*, *Tgfb*, *Il1a*, and *Il10*. Among these cytokines, the level of *Ifng* was elevated in DT-treated mice, whereas the rest were left unchanged (Fig. 6D). Because the magnitude of IL-17 versus FOXP3 in mucosal sites was shown to represent the immunological equilibrium of

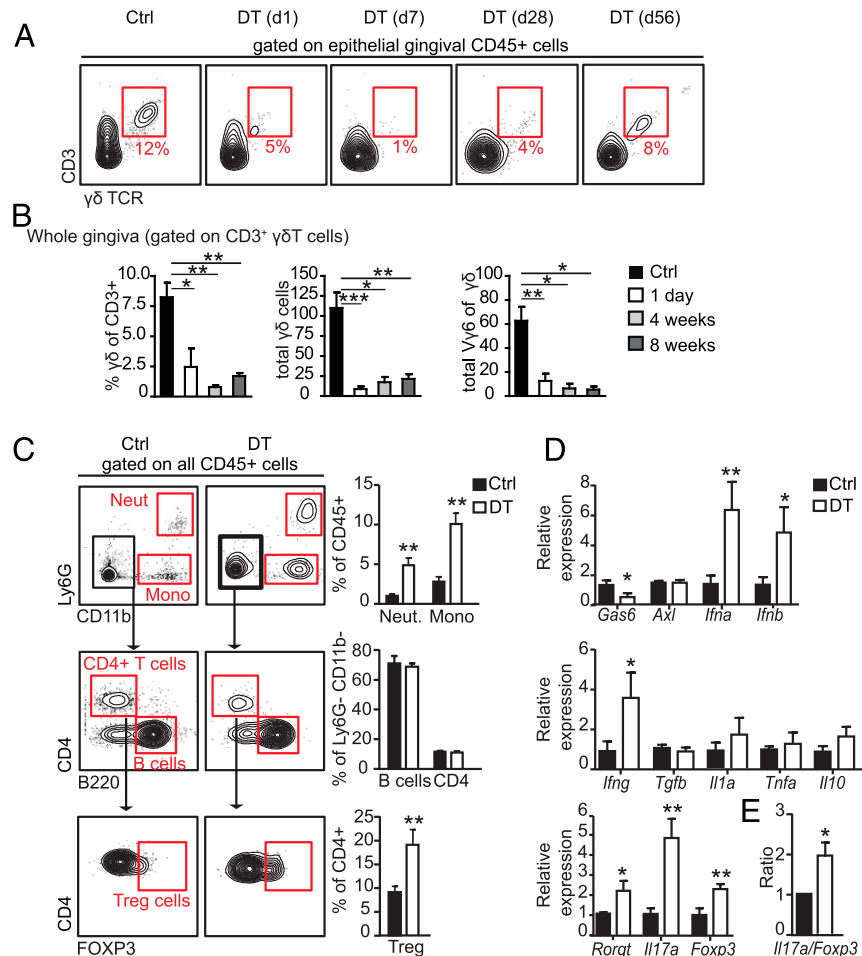


Fig. 6. Prolonged ablation of $\gamma\delta$ T cells increases gingival inflammation. (A) Repopulation kinetics of $\gamma\delta$ T cells in the gingiva and ear skin following single administration of DT to *Tcrd-GDL* mice. FACS plots demonstrate the frequencies of epithelial $\gamma\delta$ T cells; at least three mice were analyzed at each time point. (B) Bar graphs represent the mean + SEM of pooled data from three independent experiments ($n = 4$ –10 mice per experiment) of frequencies of $\gamma\delta$ T cells among CD3 as well as total numbers of $\gamma\delta$ T cells and Vy6⁺ $\gamma\delta$ T cells in the gingiva. Three to 10 mice were analyzed at each time point. (C and D) Adult *Tcrd-GDL* mice were injected intraperitoneally with DT on a weekly basis for 5 mo; gingival tissues were then collected and analyzed. (C) Representative FACS plots and graphs demonstrate the alterations in the frequencies of various leukocytes subsets in the gingiva due to the absence of $\gamma\delta$ T cells. (D) Relative expression of the indicated genes was quantified by qRT-PCR. Graphs present the transcript levels normalized to control group (Ctrl) depicted as the mean values + SEM ($n = 5$ –6). (E) *Il17a*/*Foxp3* expression level ratio in DT-treated and control groups presented as the mean values + SEM ($n = 5$). Representative data of two independent experiments are presented. * $P < 0.05$, ** $P < 0.01$, *** $P < 0.001$.

the tissue (32, 33), we also measured their relative expression. Elevated mRNA levels of *Il17a*, *Foxp3*, as well as the mRNA of *Rorgt*, a transcription factor controlling IL-17 secretion, were found in DT-treated mice (Fig. 6D). Such elevated secretion of IL-17 is likely to be mediated by other leukocytes, in line with our finding using tamoxifen-treated *Indu-Rag1* × *Tcrd-H2BeGFP* mice (Fig. 3 C–E). Furthermore, the ratio of *Il17a* versus *Foxp3* expression was almost two times higher in DT-treated mice in comparison with control mice (Fig. 6E). This suggests that, while $\gamma\delta$ T cells are the principal producers of gingival IL-17A in normal mice (Fig. 2D), other CD45⁺ cells were covering up this task after their depletion in a less balanced manner. Collectively, conditional ablation of $\gamma\delta$ T cells results in an elevated inflammation in the gingiva, suggesting an important role for these cells in regulating immunological homeostasis in the oral mucosa.

The Absence of $\gamma\delta$ T Cells Induces Oral Microbial Dysregulation. Because alteration in oral mucosal immunity is likely to affect local microbiota, we examined whether the prolonged ablation of $\gamma\delta$ T cells induced changes in the load and diversity of oral microbiota. To avoid nonspecific microbial variations, aged and sex-matched *Tcrd-GDL* mice were housed under similar conditions, before randomly dividing the mice into DT or PBS-treated groups that were housed later in separate new sterile cages. The oral microbiota was probed in these groups of mice after 5 mo of treatment by extracting DNA from oral swabs, and the ratio of ribosomal 16S/18S genes was calculated to compare the total bacterial load. As depicted in Fig. 7A, we found no alteration in the overall load of oral bacteria between the two groups. To examine if prolonged ablation of $\gamma\delta$ T cells affected bacterial diversity, we performed a taxonomic analysis of the oral micro-

biota. Indeed, significant changes in the composition of oral microbiota were detected between DT-treated mice and control mice (Fig. 7B and C). α -Diversity analysis indicated higher taxa richness in DT-treated *Tcrd-GDL* mice compared with controls (Fig. 7D), while the taxa presented in these mice significantly varied as indicated by unweighted β -diversity (Fig. 7E). Specifically, among the high-abundance bacterial families, the *Lactobacillaceae* family (*Firmicutes* phylum) was significantly increased in DT-treated mice (Fig. 7B and C and *SI Appendix*, Fig. S7A). The *Streptococcaceae* family (*Firmicutes* phylum) was not altered by the depletion of $\gamma\delta$ T cells, whereas the *Pasteurellaceae* family was reduced (*Proteobacteria*). Within the low-abundance families, a significant increase in the levels of various families was observed in the absence of $\gamma\delta$ T cells, among them the *Porphyromonadaceae* family (*Bacteroidetes*), which include the inflamophilic oral pathogen *Porphyromonas gingivalis* (6) (*SI Appendix*, Fig. S7B). Of note, further analysis revealed that the microbial dysregulation appeared after the immunological shift in the gingiva. Ten days after $\gamma\delta$ T cell depletion expression of proinflammatory genes was altered, whereas no changes were observed in the oral microbiota (*SI Appendix*, Fig. S7 C and D).

Because oral microbial shift and elevated gingival inflammation are associated with an accelerated level of spontaneous alveolar bone loss (7), we analyzed bone resorption in our system. First, we quantified the mRNA levels of *Rankl* (receptor activator of NF- κ B ligand) and *Opg* (osteoprotegerin), which are known to promote or prevent bone resorption, respectively (34). As depicted in Fig. 7F, both molecules were equally overexpressed in the tissues of DT-treated and control groups, suggesting that bone remodeling was not altered. In line with this expression pattern, bone loss could not be found in the alveolar

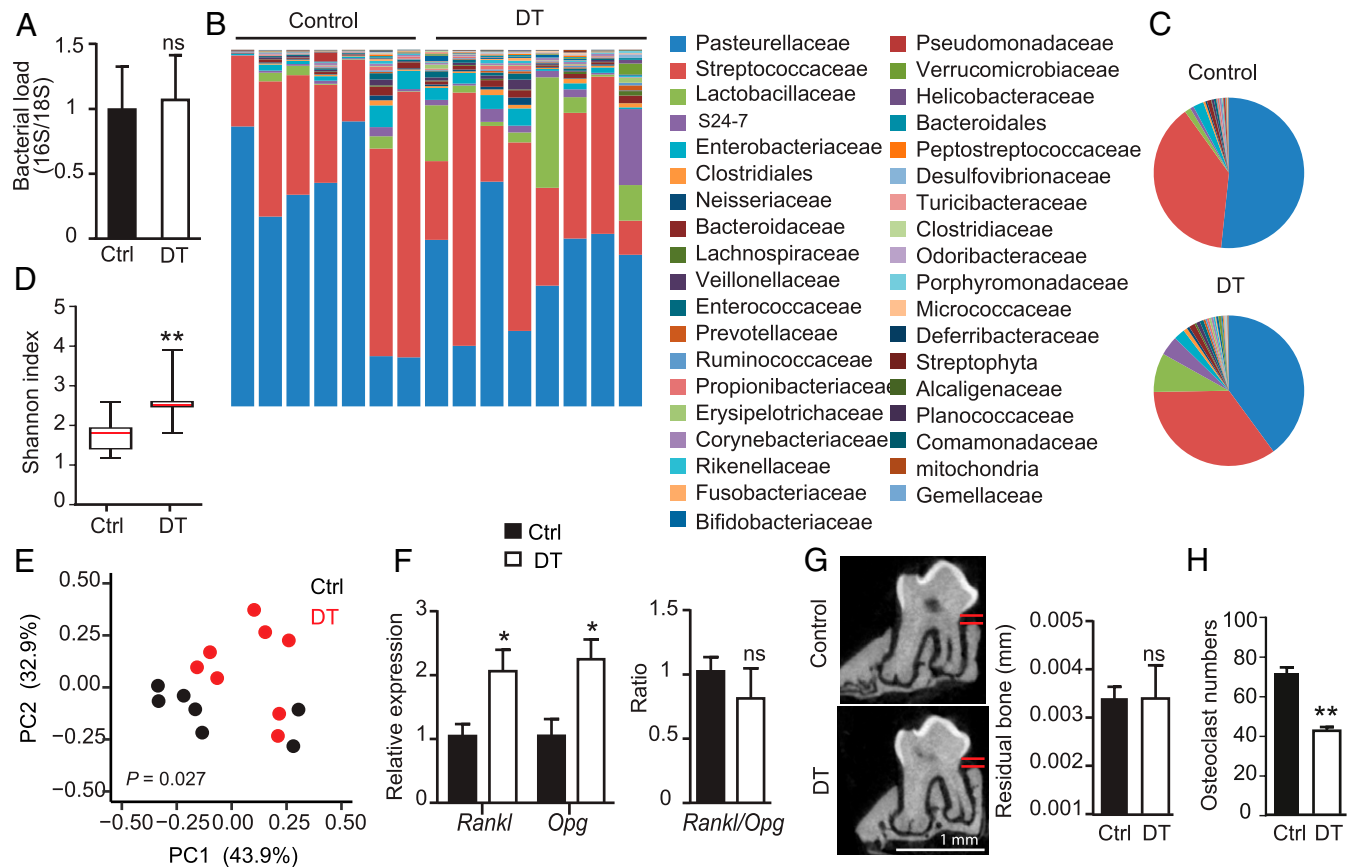


Fig. 7. Ablation of $\gamma\delta$ T cells alters the relative diversity of oral microbiota. Adult *Tcrd-GDL* mice were injected intraperitoneally with DT on a weekly basis for 5 mo. (A) Total oral bacterial load was determined in oral swabs taken from the mice by qRT-PCR of the 16S rRNA gene. Bar graphs present the 16S/18S ratio in each group as the mean values + SEM ($n = 7$ –8 per group). (B–E) Relative abundance of taxa in oral swabs sampled from DT-treated adult *Tcrd-GDL* mice and controls (Ctrl) upon prolonged DT treatment. Histograms represent the distribution of sequences in operational taxonomic units (OTUs) assigned to each class. Histograms for individual mice (B) as well as pie charts representing the mean distribution of OTU (C) are provided. (D) α -diversity plot representing taxa richness in samples of both groups of mice (rarified to 10,000 reads). Data represent the mean values + SEM ($n = 7$ –8 mice per group). (E) Principal coordinates analysis of weighted UniFrac distances based on 16S rRNA of DT-treated mice versus littermate control. Taxonomic data from one of two independent experiments are shown. (F) Relative expression of *Rankl* and *Opg* as well as *Rankl/Opg* ratio in DT treated and control mice depicted as the mean values + SEM ($n = 5$). (G) Representative μ CT sections of the second upper molar indicate the distance between the cementoenamel junction and alveolar bone crest. Graph demonstrates 3D quantification of the residual alveolar bone volume 5 mo after DT treatment presented as the mean values + SEM ($n = 6$ –7 per group). (H) Osteoclast numbers identified as tartrate-resistant acid phosphatase-positive cells in gingival sections taken from DT and control groups 2 wk after the treatment. Representative bone loss data of two independent experiments are shown. * $P < 0.05$, ** $P < 0.01$.

bone by 3D analysis using μ CT (Fig. 7G). Moreover, we found reduced osteoclast numbers around the alveolar bone as early as 2 wk after DT treatment (Fig. 7H), suggesting that $\gamma\delta$ T cells regulate osteoclast development. Taken together, these data suggest that inducible ablation of $\gamma\delta$ T cells altered microbial richness and diversity in the oral cavity. Although such microbial dysregulation, together with the elevated inflammation described earlier (Fig. 6 C and D), are expected to facilitate periodontal destruction, spontaneous alveolar bone loss was not increased due to the absence of $\gamma\delta$ T cells.

Discussion

This study characterized $\gamma\delta$ T cells of the gingiva, an immunologically challenging tissue monitoring the persistent dental biofilm and preserving oral homeostasis. Our complementary data, which were independently obtained in two different laboratories with similar results, demonstrate that mutual interplay between activated $\gamma\delta$ T cells and the microbiota shapes gingival homeostasis. First, *in vivo* ablation of $\gamma\delta$ T cells altered gingival immunity and caused microbial shift in the oral cavity. Second, the majority of intraepithelial $\gamma\delta$ T cells are localized in the junctional epithelium, in which they can get access to suprabasal layers close to the dental biofilm. Third, the frequencies of

$\gamma\delta$ T cells but not $\alpha\beta$ T cells were reduced in GF mice, as well as their ability to secrete IL-17. Moreover, the substantial loss of $V\gamma 6^+$ $\gamma\delta$ T cells observed in the gingiva of GF mice, while $V\gamma 4^+$ $\gamma\delta$ T cells were unaffected, demonstrated the capacity of the microbiota to shape gingival $\gamma\delta$ T cell subsets. In contrast to the gingiva, the microbiota has little or no impact on the homeostasis of both intestinal and skin intraepithelial $\gamma\delta$ T cells (35, 36). Nevertheless, akin to the gingiva, the microbiota plays an important role in the activation of these cells in both compartments (12, 36). Thus, the gingiva represents a unique site in which homeostatic development of intraepithelial $\gamma\delta$ T cells is clearly modulated by the microbiota. This is in line with a study reporting reduced levels of IL-17-producing $\gamma\delta$ T cells in the cervical lymph nodes of GF mice, by a mechanism involving cell-to-cell contact between $\gamma\delta$ T cells and CD103⁺ dendritic cells (37). Interestingly, we demonstrated previously that CD103 is also expressed by a subset of mucosal LCs, a special type of dendritic cell located in the gingival epithelium (9). Moreover, the frequencies of these gingival CD103⁺ LCs are specifically reduced in GF or antibiotic-treated mice, and ablation of LCs alters the load and diversity of the oral microbiota (8). Because gingival LCs mainly reside in the junctional epithelium in close proximity to intraepithelial $\gamma\delta$ T cells, it is likely that CD103⁺ LCs

represent the genuine dendritic cell subset interacting with and regulating the development of intraepithelial gingival $\gamma\delta$ T cells.

Whereas intraepithelial (dendritic) $\gamma\delta$ T cells of the skin uniquely express $V\gamma 5$, we found that $\gamma\delta$ T cells in the gingival epithelium rather resembled dermal $\gamma\delta$ T cells and were mainly $V\gamma 6^+$, but to some extent expressed also $V\gamma 1$ and $V\gamma 4$. This could be attributed, in part, to the accessibility of the gingival epithelium to circulating $V\gamma 1^+$ and $V\gamma 4^+$ cells that keep developing after birth (15). It is also conceivable that the entry of $\alpha\beta$ T cells to the gingival epithelium impacts local $\gamma\delta$ T cell frequencies. However, upon irradiation, $\gamma\delta$ T cells only slowly repopulated the gingival epithelium and host-derived cells out-competed donor-derived $\gamma\delta$ T cells in these experiments. $V\gamma 6^+$ cells probably constituted the majority of these host-derived $\gamma\delta$ T cells as they were shown to be radioresistant, while the radiosensitive $V\gamma 4^+$ cells likely originated from the donor bone marrow, as reported previously in the skin dermis (38, 39). The repopulation advantage of host-derived $V\gamma 6^+$ cells was proposed to stem from their capacity to proliferate directly in the tissue, whereas $V\gamma 4^+$ cells cannot do so (40). $V\gamma 6^+$ cells were also reported to express CCR6 (26); thus, the observed reduction of $\gamma\delta$ T cells in the gingiva of CCR6-deficient mice may be attributed, in part, to a decrease of $V\gamma 6^+$ cells. This suggests that $V\gamma 1^+$ and $V\gamma 4^+$ T cells generated after birth cannot compensate the absence of embryonic $V\gamma 6^+$ cells. Notably, the reduced numbers of $\gamma\delta$ T cells that we detected in Tamoxifen-treated *Induc-Rag1* \times *TcrdH2BeGFP* and *IL23R^{gfp/gfp}* mice confirmed the hypothesis that tissue-resident IL-17-producing $V\gamma 6^+$ cells are a major population of $\gamma\delta$ T cells in the gingival mucosa. This is also supported by the slow repopulation kinetics detected upon *in vivo* depletion, because $V\gamma 6^+$ cells are not generated in adult mice. An additional support to this assumption is that following 6 wk of parabiosis, about half of gingival $\gamma\delta$ T cells were replaced in each parabiont, indicating that $\gamma\delta$ T cells developed in adult mice can replace only non- $V\gamma 6$ cells. Furthermore, the inability of such circulating cells to fully restore gingival $\gamma\delta$ T cells 8 wk after depletion and as late as 1 y after irradiation, strongly suggested that they cannot compensate the loss or absence of $V\gamma 6^+$ cells. Thus, we propose that embryonic $V\gamma 6^+$ cells and adult $V\gamma 1^+$ and $V\gamma 4^+$ are independently maintained in the gingiva throughout life. The observed peak of $V\gamma 6^+$ cell numbers and frequencies after weaning may be in part due to increased mechanical stress and mucosal tissue injury due to mastication, as described for gingival Th17 cells (5). However, the sharp decline of $V\gamma 6^+$ cells in GF mice compared with SPF mice in two independent GF facilities, would strongly advocate for a cardinal role of the oral microbiota in maintaining gingival $\gamma\delta$ T cell homeostasis.

Interestingly, a recent work reported that $V\gamma 4^+$ and $V\gamma 1^+$ rather than $V\gamma 6^+$ cells are the major subsets of $\gamma\delta$ T cells in adult gingiva, while the majority of gingival $\gamma\delta$ T cells are radiosensitive (41). These observations contradict our data and could be simply explained by differences in the microbiota or housing conditions, such as diet, which was shown to increase the frequencies of the radiosensitive $V\gamma 4^+$ and $V\gamma 1^+$ subsets (41). However, the complementary data obtained independently by two different laboratories in the present study suggest that other factors could lead to these opposing results. For example, in the study of Krishnan et al. (41), the $V\gamma$ subsets characterized in adult gingiva represent only 55% of total $\gamma\delta$ T cells, whereas in our study above 97% of these cells were identified. It is possible that the frequencies of $V\gamma 6^+$ cells were underestimated by Krishnan et al., due to the very delicate staining protocol required to identify this particular subset. Indeed, our parabiosis, chimera, and tamoxifen-induced *Rag1* expression experiments strongly indicate that embryonic-derived $V\gamma 6^+$ cells represent the majority of gingival $\gamma\delta$ T cells in adult mice. Furthermore, the use of *TcrdH2BeGFP* reporter mice allowed us to identify more precisely the $\gamma\delta$ T cells compared with staining with GL3 antibody. An additional major difference between both studies is related to the impact of the microbiota on gingival $\gamma\delta$ T cells. Krishnan et al. reported no alteration in the composition of the $V\gamma$ subsets in GF mice, al-

though the total numbers of gingival $\gamma\delta$ T cells were reduced compared with SPF mice. We similarly revealed a decrease in gingival $\gamma\delta$ T cells, which was attributed to a significant reduction of the $V\gamma 6^+$ subset. This is in agreement with a recent study reporting that oral microbiota expanded IL-17-producing $V\gamma 6^+$ cells systemically (37). Unfortunately, Krishnan et al. did not examine the $V\gamma 6^+$ cells in GF mice and, moreover, they limited their analysis to the first week after birth, which might cloak the large impact of the microbiota on $V\gamma 6^+$ cells.

Conditional ablation of $\gamma\delta$ T cells resulted in an elevated gingival inflammation and significant modifications in the diversity of oral microbiota. Similar microbial changes were reported in IL17R-deficient mice, demonstrating expansion of *Lactobacillus*, reduction of *Pasteurellaceae*, while *Streptococcaceae* was not affected (37). This further supports the importance of steady-state IL-17 signaling by $\gamma\delta$ T cells, the main IL-17-producing cells in the oral mucosa. Interestingly, in contrast to these observations, in *Tcrd*^{−/−} mice no change was found in the load and richness of oral microbiota compared with wild-type mice; however, an overgrowth of *Aggregatibacter* species was reported (41). This echoes the fundamental difference between *Tcrd*^{−/−} mice and *Tcrd-GDL* mice with regards to the impact of $\gamma\delta$ T cells on the homeostasis of oral microbiota (42). Other lymphocytes developing in the empty niche of genuine $\gamma\delta$ T cells in *Tcrd*^{−/−} mice might be less suited to balance gingival homeostasis, possibly because they cannot produce regulatory factors, such as Areg in addition to proinflammatory IL-17 (41), and thereby facilitate periodontal bone loss. In any case, expansion of *Lactobacillaceae* directly reflects the immunological status of the gingiva of $\gamma\delta$ T cells-depleted mice, because this family is capable of using inflammation byproducts for anaerobic respiration facilitating their growth in an inflamed environment (43–45). This could also explain the outgrowth of *Aggregatibacter* species in *Tcrd*^{−/−} mice, although the immunological status of the gingiva in these mice was not addressed by Krishnan et al. (41).

We have recently shown a similar shift in the oral microbiota using *Gas6*^{−/−} mice, a key homeostatic regulator of the oral mucosa (7), which was also down-regulated in the present study upon depletion of $\gamma\delta$ T cells. Such activity of GAS6 involved down modulation of IFN I signaling in mucosal tissues (7, 46), and the substantial elevation of *Ifna/b* mRNA levels in $\gamma\delta$ T cell-depleted mice suggest that this regulatory pathway is also affected in our system. Of note, the *Porphyromonadaceae* family was also augmented in the absence of $\gamma\delta$ T cells. This is highly relevant to oral health, as this family includes the keystone oral pathogen *P. gingivalis* that flourishes in periodontal inflammation and is closely associated with tissue destruction (6). Nevertheless, despite the higher gingival inflammation and microbial dysregulation observed in $\gamma\delta$ T cell-depleted mice, which are strongly associated with destructive immunity (1), we did not observe an accelerated alveolar bone loss. This could be explained by our findings that the bacterial load and RANKL/OPG ratio were not altered upon depletion, suggesting that the nature of gingival inflammation rather than its magnitude is relevant for the alveolar bone loss process. Alternatively, the reduction in osteoclast numbers around the alveolar bone suggests that $\gamma\delta$ T cells might regulate osteoclast differentiation regardless to the overall inflammatory level of the gingiva. However, the overall lack of effect on the alveolar bone might suggest that bone resorption activity of the residual osteoclasts is increased due to local inflammation (47), thus compensating the reduction in their numbers. It is also possible that depletion of $\gamma\delta$ T cells is affecting osteoblasts, because osteoblast function was shown to be compromised under inflammatory conditions and therefore bone formation is decreased (48).

In contrast to our study, a recent work employing *Tcrd*^{−/−} mice reported that $\gamma\delta$ T cells are essential for protection against age-associated periodontal bone loss (41). Nevertheless, *Tcrd*^{−/−} mice, unlike the *Tcrd-GDL* mice used in our study, lack $\gamma\delta$ T cells during pre- and postnatal development, and it is likely that *Tcrd*^{−/−} mice compensate the loss of these cells by recruiting

other effector cells to the gingiva. Indeed, we showed recently that the lack of $\gamma\delta$ T cells in constitutive *Tcrd*^{-/-} mice is functionally compensated by other lymphocytes taking over genuine $\gamma\delta$ T cell functions (42). Additionally, we demonstrate here that ablation of embryonic-derived $\gamma\delta$ T cells resulted in a development of other IL-17-expressing leukocytes. These might be less suited to balance gingival homeostasis, possibly because they can produce regulatory factors, such as Areg, in addition to proinflammatory IL-17 (41), and thereby facilitate periodontal bone loss. *Tcrd-GDL* mice, on the other hand, develop normally and thus represent more adequately the role of $\gamma\delta$ T cells in age-associated bone loss. It should be mentioned that the lack of effect on bone volume in *Tcrd-GDL* mice could not be explained by an insufficient depletion period of only 8 wk, because we and others have reported that natural bone loss can be detected during this time (2, 8).

In conclusion, this study demonstrates the subtle and critical role of gingival intraepithelial $\gamma\delta$ T cells in oral mucosal homeostasis. This task is mediated by $\gamma\delta$ T cells developing both pre- and postnatally, which are maintained independently in the tissue. Furthermore, the development and homeostasis of gingival $\gamma\delta$ T cells is shaped by the microbiota, a unique phenomenon that does not occur in the intestine and skin epithelia to this extent. Therefore, targeting $\gamma\delta$ T cells is a promising strategy to modulate and improve oral health.

1. Moutsopoulos NM, Konkel JE (2018) Tissue-specific immunity at the oral mucosal barrier. *Trends Immunol* 39:276–287.
2. Hajishengallis G (2015) Periodontitis: From microbial immune subversion to systemic inflammation. *Nat Rev Immunol* 15:30–44.
3. Greer A, Zenobia C, Darveau RP (2013) Defensins and LL-37: A review of function in the gingival epithelium. *Periodontol 2000* 63:67–79.
4. Eskan MA, Rose BG, Benakanakere MR, Lee MJ, Kinane DF (2008) Sphingosine 1-phosphate 1 and TLR4 mediate IFN- β expression in human gingival epithelial cells. *J Immunol* 180:1818–1825.
5. Dutzan N, et al. (2017) On-going mechanical damage from mastication drives homeostatic Th17 cell responses at the oral barrier. *Immunity* 46:133–147.
6. Hajishengallis G, et al. (2011) Low-abundance biofilm species orchestrates inflammatory periodontal disease through the commensal microbiota and complement. *Cell Host Microbe* 10:497–506.
7. Nassar M, et al. (2017) GAS6 is a key homeostatic immunological regulator of host-commensal interactions in the oral mucosa. *Proc Natl Acad Sci USA* 114:E337–E346.
8. Capucha T, et al. (2018) Sequential BMP7/TGF- β 1 signaling and microbiota instruct mucosal Langerhans cell differentiation. *J Exp Med* 215:481–500.
9. Capucha T, et al. (2015) Distinct murine mucosal Langerhans cell subsets develop from pre-dendritic cells and monocytes. *Immunity* 43:369–381.
10. Chien YH, Meyer C, Bonneville M (2014) $\gamma\delta$ T cells: First line of defense and beyond. *Annu Rev Immunol* 33:121–155.
11. Conti HR, et al. (2014) Oral-resident natural Th17 cells and $\gamma\delta$ T cells control opportunistic *Candida albicans* infections. *J Exp Med* 211:2075–2084.
12. Nielsen MM, Witherden DA, Havran WL (2017) $\gamma\delta$ T cells in homeostasis and host defence of epithelial barrier tissues. *Nat Rev Immunol* 17:733–745.
13. Carding SR, Egan PJ (2002) Gammadelta T cells: Functional plasticity and heterogeneity. *Nat Rev Immunol* 2:336–345.
14. Prinz I, Silva-Santos B, Pennington DJ (2013) Functional development of $\gamma\delta$ T cells. *Eur J Immunol* 43:1988–1994.
15. Haas JD, et al. (2012) Development of interleukin-17-producing $\gamma\delta$ T cells is restricted to a functional embryonic wave. *Immunity* 37:48–59.
16. Sumaria N, et al. (2011) Cutaneous immunosurveillance by self-renewing dermal gammadelta T cells. *J Exp Med* 208:505–518.
17. Zeng S, et al. (2014) Infection with respiratory syncytial virus influences FasL-mediated apoptosis of pulmonary $\gamma\delta$ T cells in a murine model of allergen sensitization. *J Asthma* 51:360–365.
18. Zeng X, et al. (2012) $\gamma\delta$ T cells recognize a microbial encoded B cell antigen to initiate a rapid antigen-specific interleukin-17 response. *Immunity* 37:524–534.
19. Edelblum KL, et al. (2015) $\gamma\delta$ T cell intraepithelial lymphocyte migration limits transepithelial pathogen invasion and systemic disease in mice. *Gastroenterology* 148:1417–1426.
20. Chowdhury AC, Chaurasia S, Mishra SK, Aggarwal A, Misra R (2017) IL-17 and IFN- γ producing NK and $\gamma\delta$ T cells are preferentially expanded in synovial fluid of patients with reactive arthritis and undifferentiated spondyloarthritis. *Clin Immunol* 183:207–212.
21. Ramirez-Valle F, Gray EE, Cyster JG (2015) Inflammation induces dermal V γ 4+ $\gamma\delta$ T17 memory-like cells that travel to distant skin and accelerate secondary IL-17-driven responses. *Proc Natl Acad Sci USA* 112:8046–8051.
22. Kuziel WA, et al. (1987) Regulation of T-cell receptor gamma-chain RNA expression in murine Thy-1+ dendritic epidermal cells. *Nature* 328:263–266.
23. McGeechey MJ, et al. (2009) The interleukin 23 receptor is essential for the terminal differentiation of interleukin 17-producing effector T helper cells in vivo. *Nat Immunol* 10:314–324.
24. Stritesky GL, Yeh N, Kaplan MH (2008) IL-23 promotes maintenance but not commitment to the Th17 lineage. *J Immunol* 181:5948–5955.
25. Fraticelli P, et al. (2001) Fractalkine (CX3CL1) as an amplification circuit of polarized Th1 responses. *J Clin Invest* 107:1173–1181.
26. Haas JD, et al. (2009) CCR6 and NK1.1 distinguish between IL-17A and IFN-gamma-producing gammadelta effector T cells. *Eur J Immunol* 39:3488–3497.
27. Hirota K, et al. (2007) Preferential recruitment of CCR6-expressing Th17 cells to inflamed joints via CCL20 in rheumatoid arthritis and its animal model. *J Exp Med* 204:2803–2812.
28. Yoneda O, et al. (2003) Membrane-bound form of fractalkine induces IFN-gamma production by NK cells. *Eur J Immunol* 33:53–58.
29. Düber S, et al. (2009) Induction of B-cell development in adult mice reveals the ability of bone marrow to produce B-1a cells. *Blood* 114:4960–4967.
30. Liang S, Hosur KB, Domon H, Hajishengallis G (2010) Periodontal inflammation and bone loss in aged mice. *J Periodontal Res* 45:574–578.
31. Arizon M, et al. (2012) Langerhans cells down-regulate inflammation-driven alveolar bone loss. *Proc Natl Acad Sci USA* 109:7043–7048.
32. Wan YY, Flavell RA (2007) Regulatory T-cell functions are subverted and converted owing to attenuated Foxp3 expression. *Nature* 445:766–770.
33. Lochner M, et al. (2008) In vivo equilibrium of proinflammatory IL-17+ and regulatory IL-10+ Foxp3+ RORgamma t+ T cells. *J Exp Med* 205:1381–1393.
34. Cochran DL (2008) Inflammation and bone loss in periodontal disease. *J Periodontol* 79(Suppl 8):1569–1576.
35. Bandeira A, et al. (1990) Localization of gamma/delta T cells to the intestinal epithelium is independent of normal microbial colonization. *J Exp Med* 172:239–244.
36. Naik S, et al. (2012) Compartmentalized control of skin immunity by resident commensals. *Science* 337:1115–1119.
37. Fleming C, et al. (2017) Microbiota-activated CD103⁺ DCs stemming from microbiota adaptation specifically drive $\gamma\delta$ T17 proliferation and activation. *Microbiome* 5:46.
38. Gray EE, Suzuki K, Cyster JG (2011) Cutting edge: Identification of a motile IL-17-producing gammadelta T cell population in the dermis. *J Immunol* 186:6091–6095.
39. Cai Y, et al. (2014) Differential developmental requirement and peripheral regulation for dermal V γ 4 and V γ 6T17 cells in health and inflammation. *Nat Commun* 5:3986, and erratum (2016) 7:11354.
40. O'Brien RL, Born WK (2015) Dermal $\gamma\delta$ T cells—What have we learned? *Cell Immunol* 296:62–69.
41. Krishnan S, et al. (2018) Amphiregulin-producing $\gamma\delta$ T cells are vital for safeguarding oral barrier immune homeostasis. *Proc Natl Acad Sci USA* 115:10738–10743.
42. Sandrock I, et al. (2018) Genetic models reveal origin, persistence and non-redundant functions of IL-17-producing $\gamma\delta$ T cells. *J Exp Med* 215:3006–3018.
43. Smith PM, et al. (2013) The microbial metabolites, short-chain fatty acids, regulate colonic Treg cell homeostasis. *Science* 341:569–573.
44. Winter SE, et al. (2010) Gut inflammation provides a respiratory electron acceptor for *Salmonella*. *Nature* 467:426–429.
45. Winter SE, et al. (2013) Host-derived nitrate boosts growth of *E. coli* in the inflamed gut. *Science* 339:708–711.
46. Gough DJ, Messina NL, Clarke CJ, Johnstone RW, Levy DE (2012) Constitutive type I interferon modulates homeostatic balance through tonic signaling. *Immunity* 36:166–174.
47. Mbalaviele G, Novack DV, Schett G, Teitelbaum SL (2017) Inflammatory osteolysis: A conspiracy against bone. *J Clin Invest* 127:2030–2039.
48. Walsh NC, et al. (2009) Osteoblast function is compromised at sites of focal bone erosion in inflammatory arthritis. *J Bone Miner Res* 24:1572–1585.

Materials and Methods

All animal protocols were approved by the Hebrew University Institutional Animal Care and Use Committee as well as in accordance with institutional guidelines of the Hannover Medical School, approved by the Lower Saxony State Office for Consumer Protection and Food Safety animal care and use committee. GF or SPF adult B6 mice were maintained in sterile isolators at the Weizmann Institute or at the central animal facility at Hannover Medical School, the studies were approved by the Institutional Animal Care and Use Committee of the Weizmann Institute of Science or Hannover Medical School, respectively.

Detailed information on antibodies, reagents, mice, and ethical approvals is described in *SI Appendix*. Details of parabiosis experiments, chimeric mice, immunofluorescence staining, isolation, and processing of gingival and skin $\gamma\delta$ T cells, two-photon microscopy, conditional ablation of $\gamma\delta$ T cells in vivo, RNA extraction, and qRT-PCR, induction of Rag1 enzyme expression in adult mice, BrdU incorporation assays, microbiota analysis, bone loss quantification, and statistical analysis are provided in *SI Appendix*.

ACKNOWLEDGMENTS. We thank Tiago Amado and Bruno Silva-Santos for kindly providing *B6.129S4-1fngtm3.1Lky Il17atm1Bcgen* (MGI:5426367, here *IL17eGFP*) reporter mice. This work was supported by the German-Israeli Foundation for Scientific Research and Development Grant 1432 (to A.-H.H. and I.P.) and Deutsche Forschungsgemeinschaft Grants PR727/4-1 and SFB900-B8 (to I.P.). A. Wilharm was supported by the Hannover Biomedical Research School, and Y.T. was supported by the Faculty of Dental Medicine, Hebrew University.